

K.-V. Schubert  
K.M. Lusvardi  
E.W. Kaler

## Polymerization in nonaqueous microemulsions

Received: 23 October 1995  
Accepted: 11 March 1996

K.-V. Schubert  
E.I. DuPont de Nemours & Co.  
Central Research and Development  
P.O. Box 80356  
Wilmington, Delaware 19880-0356, USA

K.M. Lusvardi · Prof. Dr. E.W. Kaler (✉)  
Center for Molecular and Engineering  
Thermodynamics  
Department of Chemical Engineering  
University of Delaware  
Newark, Delaware 19716, USA

**Abstract** Nonaqueous microemulsions containing formamide, the anionic surfactant AOT (bis(2-ethylhexyl)sulfosuccinate sodium salt), sodium bromide (NaBr), and either of the monomers hexyl methacrylate or styrene are polymerized at 60 °C. For both monomers, the final product is a stable, bluish dispersion of particles of ca. 80 nm diameter. Based on phase behavior studies as a function of NaBr concentration, we describe how a systematic variation of composition

and monomer causes changes in reaction rates and latex characteristics. The monomer solubility in the continuous phase plays an important role in determining the final polymer characteristics. Decreasing monomer solubility shifts the mechanism from one similar to solution polymerization to one closer to traditional emulsion polymerization.

**Key words** Microemulsion – polymerization – nonaqueous – latex

### Introduction

Microemulsions are solutions containing at least oil, surfactant, and water or another polar compound such as formamide or propylene glycol [1–3]. They are stable and often transparent, and so differ considerably from thermodynamically unstable and usually turbid emulsions.

Polymerization reactions in microemulsions have been explored with the goals of either fixing their labile microstructure or producing latices with sizes below those normally generated by emulsion polymerization [4–10]. Microemulsions containing monomers in their oil continuous domains have been polymerized, but the microemulsion does not remain stable during the reaction [4, 5, 9, 11, 12]. Monomer-in-water microemulsions have been successfully polymerized to yield stable, bluish latex dispersions. The latex particles are larger than the original unpolymerized microemulsion droplets, but the resulting polymer has a narrow molecular weight distribution [13–15]. Water-in-oil microemulsions containing water-soluble monomers can also be polymerized to yield water-swollen polymer particles dispersed in oil [10].

Although there are numerous publications about polymerization reactions in microemulsions, there is no general theory, in part because a large number of results are so specific to certain components of the microemulsion. For example, in some cases monomers were polymerized in microemulsions containing alcohols as cosurfactants. It is known that alcohols penetrate the surfactant monolayer [16], modify monomer partitioning [17–20] between the phases, and alter the size of microemulsion aggregates [16, 21, 22]. Additionally, their presence promotes chain-transfer reactions [20] that result in polymers of lower molecular weight. Such systems are therefore not suited for discovery of the fundamental parameters governing the kinetics and the properties of the final latex.

One step towards a quantitative microscopic description is to vary systematically the type of monomer and the composition in a model microemulsion system. An essential preliminary step is a systematic phase behavior study with the goal of reducing the number of components to the minimum of water, monomer and surfactant. Achieving this goal, however, is not easy. Such model microemulsions can be made if a nonionic surfactant is used [23, 24], but unfortunately nonionic surfactants are ether compounds

and have a terminal hydroxyl group. Thus nonionic surfactants are likely chain transfer agents [25]. Microemulsions can be made with ionic surfactants without the use of alcohols, either by finding a well-suited ionic surfactant that microemulsifies the monomer in the desired region of the phase diagram [14, 26–28], or by using mixtures of surfactants [13, 29–31] or, as is the focus here, by using nonaqueous microemulsions.

Microemulsions form when water is replaced by the polar protic solvent formamide ( $\text{HCONH}_2$ ). This solvent has a very high dielectric constant, a high cohesive energy, and forms hydrogen bonds. Generally, the phase behavior of surfactants in formamide follows the same generic pattern found with aqueous solutions [3, 32, 33]. The only major difference is a decrease in the efficiency of the surfactants when used in formamide. Nonaqueous microemulsions with ionic surfactants form without adding cosurfactants [3].

Here we report a novel microemulsion polymerization of a nonaqueous microemulsion. Such mixtures enable us to investigate how reaction rates and polymer characteristics depend on composition, reaction conditions, and the monomer solubility in the continuous phase.

## Experimental

### Materials

Formamide (FA) ( $\text{HCONH}_2$ ) was purchased from Fluka in the highest quality available (puriss p.a. > 99.0%) and used as received. AOT (bis(2-ethylhexyl)sulfosuccinate sodium salt) and NaBr were also from Fluka in MicroSelect quality. AOT was used after drying under vacuum at 60 °C for 24 h and NaBr was used as received. The monomers (oils) styrene and hexyl methacrylate (denoted as C6MA) were purchased from Scientific Polymer Products, Inc. and were vacuum distilled to remove the inhibitor and any oligomers. Distilled monomers were stored at 2 °C and were used within several days. The initiator potassium persulfate (KPS) was purchased from Aldrich with a quoted purity of 99.99% and was used as received. The initiator was stored at 2 °C.

Composition of samples in terms of masses  $m_i$  are calculated as follows: Surfactant concentration ( $\gamma$ ) with  $\gamma = m_{\text{AOT}}/(m_{\text{FA}} + m_{\text{oil}} + m_{\text{NaBr}} + m_{\text{AOT}})$ ; oil concentration ( $\alpha$ ) with  $\alpha = m_{\text{oil}}/(m_{\text{FA}} + m_{\text{oil}})$ ; salt concentration ( $\epsilon$ ) with  $\epsilon = m_{\text{NaBr}}/(m_{\text{FA}} + m_{\text{NaBr}})$  or in mM NaBr, (based on the polar solvent) and initiator concentration with KPS =  $(m_{\text{KPS}}/m_{\text{KPS}} + m_{\text{oil}})$ . Note that the initiator concentration given in wt% is based on the oil content. For a better comparison with literature data, however, it is also reported in mol/l polar solvent.

### Phase behavior

The phase behavior was studied at constant temperature as a function of electrolyte concentration. Samples with equal amounts of formamide and oil and high surfactant concentrations were prepared, heated to 60 °C, and equilibrated. To determine phase boundaries, these samples were then diluted with equal volumes of oil and a concentrated NaBr solution in formamide. Phase diagrams at constant surfactant concentration were determined by mixing stock solutions of monomer and surfactant with solutions of formamide, surfactant and electrolyte.

### Polymerization

All components (typically a total of ca. 170 g) were added into a 250 ml round flask equipped with a septum port, sealed with a stopper and stirred. After the AOT dissolved the mixture remained isotropic at room temperature. In order to remove solubilized oxygen (which inhibits or retards the radical reaction), the reaction mixture was frozen in liquid nitrogen and degassed at 0.01 Torr for three freeze-thaw cycles (total period of degassing was 75 min). About 0.1% of the mass of the sample was lost during these freeze-thaw cycles. The microemulsion was then blanketed with a constant positive pressure of nitrogen. KPS (potassium persulfate) is a water-soluble initiator with a solubility of 5.2 wt% in formamide. The initiator was dissolved in a small fraction of formamide. The initiator solution was then degassed for 20 min at 0.5 Torr before it was injected with a Gilmont Syringe (with an accuracy of better than 0.01 ml) through the septum port into the reaction mixture, which was already equilibrated at 60 °C ( $\pm 0.1$  °C) in a thermostated waterbath. After removing the Gilmont syringe a needle with a syringe valve was immersed through the septum port into the reaction mixture in order to remove samples throughout the reaction without introducing oxygen.

The rate of polymerization was obtained by recording changes in the density of the mixture during the reaction. In certain intervals, samples were pulled from the mixture and immediately frozen in liquid nitrogen. After thawing, the homogenous samples were immediately injected into an Anton Paar DMA 60 densimeter equipped with a DMA 602 remote cell. All densities are measured at  $25 \pm 0.02$  °C with an accuracy of  $\pm 1.5 \times 10^{-6} \text{ g cm}^{-3}$ . Polymer precipitates from samples frozen for more than 12 h.

All conversion curves show an immediate increase in density (there is no induction period) after the initiator was injected. Repeated reactions yield the same density values. Final conversion values were obtained by gravimetry

(after adding an excess of hydroquinone to the sample) and have an accuracy of  $\pm 3\%$ .

### Molecular weights and latex diameters

In certain intervals during the reaction, 10 ml samples were removed from the reaction mixture and the polymer was immediately precipitated in 250 ml methanol (HPLC grade). After 16 h the polymer settled, the methanol was decanted, and the polymer was washed with distilled water and methanol before it was dried in a vacuum oven at 50 °C for 24 h. The polymer obtained is waxy and sticky and is sometimes transparent (the glass transition temperature for polyC6MA is approximately  $-5^\circ\text{C}$ ). Molecular weights of the polymer were determined using Size Exclusion Chromatography (SEC). Coupled detectors (low-angle laser light scattering (LALLS) and refractive index (RI), both from Polymer Laboratories) allow determination of absolute molecular weights. The mobile phase was methylethylketone (MEK, from J.T. Baker, HPLC grade) with a flow rate of 1 ml/min and the polymers were separated using two 30 cm "PL gel 20  $\mu$  Mixed A" columns (purchased from Polymer Laboratories). The calibration constants for the LALLS and RI detectors were determined from narrow molecular weight distribution polystyrene standards and data analysis was performed using the software provided by Polymer Labs. Typical concentrations for samples (not standards) were between 6 and 7 mg polymer per ml mobile phase. Each sample was injected twice and analysis of the traces shows that  $\bar{M}_w$  are reproduced within  $\pm 10\%$ . Polydispersity numbers ( $\bar{M}_w/\bar{M}_n$ ) given in Table 1 are only reported for samples displaying one sharp peak in the spectrum.

Latex particle diameters were determined using QLS with equipment previously described [14]. Latices were diluted 500 times to minimize particle-particle interactions and filtered through 0.8- $\mu\text{m}$  Millex Millipore filters to eliminate dust before QLS measurements. The measured diffusion coefficients were represented in terms of apparent radii by using the Stokes-Einstein relation and assuming the solvent has the viscosity of water.

## Results

### Phase behavior

The phase behavior of a quaternary system at constant temperature and ambient pressure can be represented in an upright phase prism (for a schematic see ref. [34]). The Gibbs triangle with polar solvent (A), nonpolar solvent (B) and surfactant (C) forms the base and electrolyte (D) con-

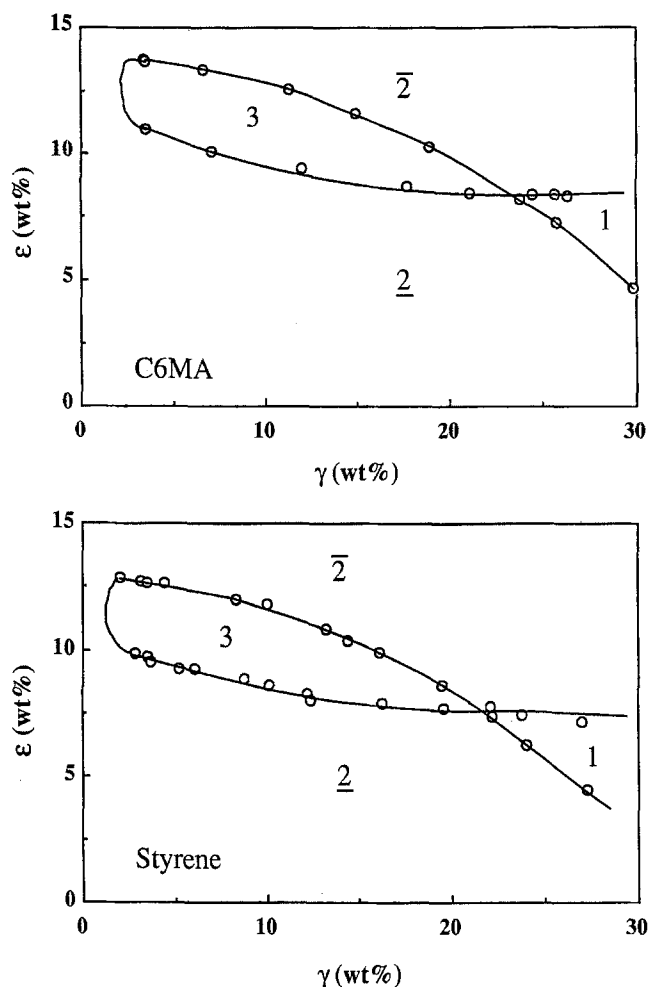
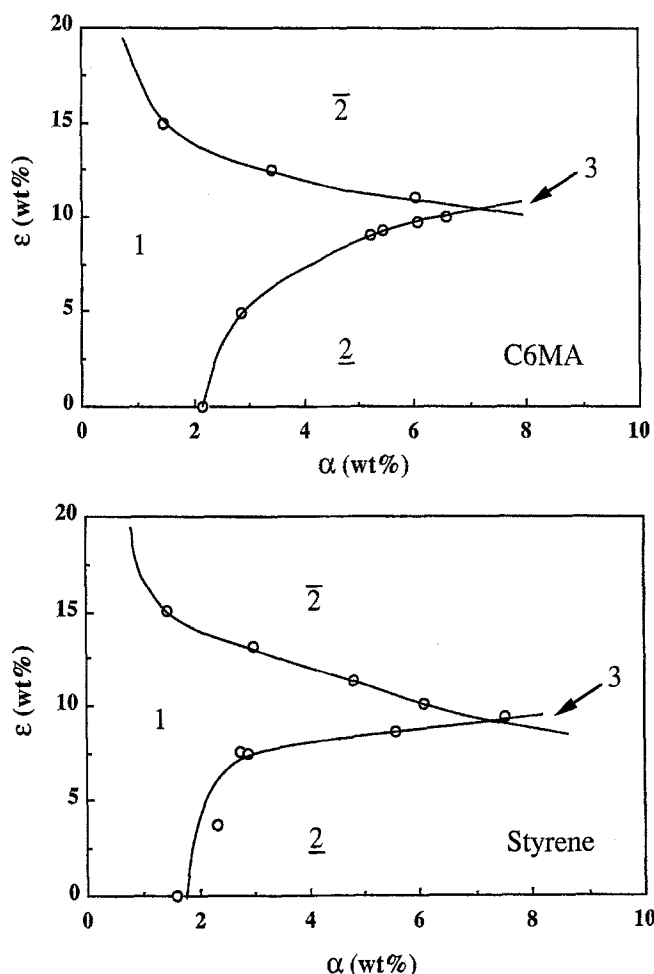


Fig. 1 Vertical sections through the phase prisms of formamide, monomer, NaBr, and AOT at equal amounts of formamide and monomer at  $T = 60^\circ\text{C}$ . C6MA (top) and styrene (bottom) are the monomers

centration ( $\varepsilon$ , with  $\varepsilon = D/(A + D)$  in wt%) is the ordinate. A vertical section through this prism at equal amounts of water and oil ( $\alpha$ , with  $\alpha = B/(A + B)$  in vol% or wt%) leads to a two-dimensional phase diagram that contains the shape of a fish (cf. Fig. 1). The fish tail region at high surfactant concentrations ( $\gamma$ , with  $\gamma = C/(A + B + C + D)$  in wt%) is the homogeneous microemulsion region. Based on knowledge of the location of the three phase body in phase space, one can study the phase behavior at a chosen constant surfactant concentration and determine how much oil can be solubilized as a function of salt concentration (cf. Fig. 2). Such diagrams are referred to as "channel cuts" in the literature [35]. Several microstructural investigations show the microemulsion in this region contains oil swollen micelles, i.e., the solution is an oil-in-water microemulsion [31, 36, 37].

Figure 1 shows the partial phase diagram of the system formamide – NaBr – monomer – AOT at 60 °C with equal



**Fig. 2** Vertical sections through the phase prisms of formamide, monomer, NaBr, and AOT at surfactant concentration,  $\gamma = 10$  wt%, at  $T = 60^\circ\text{C}$ , C6MA (top) and styrene (bottom) are the monomers

volumes of formamide and monomer. The phase behavior is nearly identical for both monomers. For example, the minimum surfactant concentration necessary to obtain a single phase is 23 wt% AOT at 8.5 wt% NaBr for C6MA and 22 wt% AOT at 7.5 wt% NaBr for styrene. At this (or at higher) surfactant concentration the phase sequence as electrolyte is increased moves from  $\underline{2}$  (oil-in-FA microemulsion phase in equilibrium with an excess oil phase), to the homogeneous microemulsion phase (1), to  $\bar{2}$  (FA-in-oil microemulsion phase in equilibrium with an excess formamide phase). At lower surfactant concentrations the phase sequence  $\underline{2} - 3 - \bar{2}$  occurs with increasing NaBr concentration. Within the three-phase region the microemulsion phase is in equilibrium with both polar and nonpolar excess phases.

To find the amount of oil that can be solubilized at a constant surfactant concentration as a function of elec-

trolyte amount, a section is erected through the phase prism at  $\gamma = 10$  wt% (this is approximately half the concentration needed to solubilize equal amounts of both polar and nonpolar phase). The phase diagrams are shown in Fig. 2. Again, the extensions of the microemulsion region in these "channel cuts" are nearly identical for both monomers. In either case, almost 2 wt% of the monomer can be solubilized in the salt-free mixture. Increasing the salt concentration leads to a larger microemulsion region, e.g. at 10 wt% NaBr either 6.5 wt% of C6MA or 6 wt% of styrene can be solubilized. Increasing electrolyte concentration ultimately leads to the so-called salting out of the surfactant into the oil-rich phase ( $\bar{2}$ ). Increasing the oil content at intermediate salt concentrations leads to a three-phase region.

It is important to note that the solubility of styrene in formamide is ca. 1 wt% at  $60^\circ\text{C}$ , whereas C6MA is significantly more solvophobic. Based on published data on solubilities of styrene and alkyl methacrylates in water and formamide [38–40], we estimate the solubility of C6MA in formamide to be ca. 0.2 wt% at  $T = 60^\circ\text{C}$ .

### Polymerization

This section is divided into three parts. First, the effect of initiator concentration on the reaction kinetics and polymer properties of the FA–C6MA–AOT ( $\gamma = 10$  wt% and  $\alpha = 1.5$  wt%) mixtures are examined. Second, the composition of the parent microemulsion system is changed to investigate changes in reaction rates and product characteristics. Finally, styrene is substituted as the monomer and polymerized in a "microemulsion" at a concentration where styrene is soluble in the polar phase. The goal of this experiment is to learn more about the effect of the monomer solubility in the polar phase on the reaction and the final product.

The polymerizations are carried out in only a rather narrow range in the microemulsion region because polymerization at relatively high electrolyte and monomer concentrations leads to precipitation of polymer during the reaction. The model C6MA microemulsion polymerization has the composition  $\alpha = 1.5$  wt%,  $\gamma = 10$  wt%,  $\varepsilon = 0\%$  and is initiated with KPS concentrations of 4.75%, 2.50% and 0.50% with respect to the oil content. This is equivalent to initiator concentrations in the polar domain of 3.18 mM, 1.64 mM and 0.32 mM, respectively. A KPS concentration of 2.50% will be the model concentration when either the microemulsion composition is changed to  $\alpha = 1.0$  wt% or a small amount of salt ( $\varepsilon = 0.05$  M NaBr) is added. Styrene will be polymerized with a composition  $\alpha = 1.0$  wt%,  $\gamma = 10$  wt%,  $\varepsilon = 0\%$ . Table 1 summarizes these results.

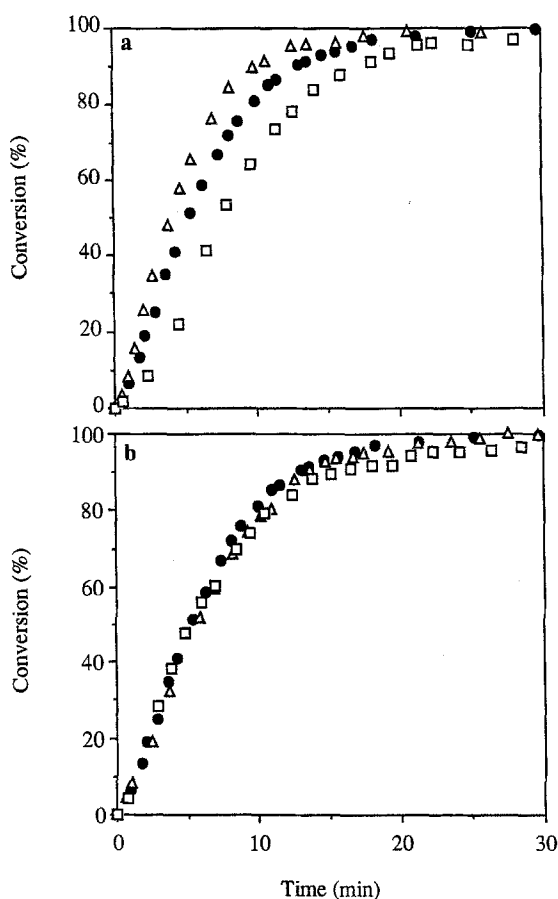


Fig. 3 Conversion as a function of time for polymerization at  $T = 60^\circ\text{C}$  of (a)  $\alpha = 1.50$  wt% C6MA with KPS concentrations of ( $\Delta$ ) 3.18 mM; ( $\bullet$ ) 1.64 mM and ( $\square$ ) 0.32 mM (b) ( $\bullet$ )  $\alpha = 1.5$  wt% C6MA with 1.64 mM KPS; ( $\Delta$ )  $\alpha = 1.5$  wt% C6MA and 0.05 M NaBr with 1.64 mM KPS; ( $\square$ )  $\alpha = 1.0$  wt% C6MA with 1.08 mM KPS

#### C6MA systems

**Effect of initiator concentration:** A nonaqueous microemulsion containing C6MA can be polymerized when initiated with KPS. The reaction mixture turns bluish while the reaction proceeds, which indicates growth of particles. The reaction is very fast for all mixtures and conversion values of 98–99% are reached, as determined by gravimetry (Fig. 3a). The increasing rate of polymerization in the early stages is attributed to the increasing number of polymer loci that are nucleated by free radicals. The decreasing rate in the later stages of the reaction is due to a diminishing monomer concentration in the growing particles. Lowering the KPS concentration from 3.18 mM to 1.64 mM slows the reaction rate, and a final conversion of 98% is reached after 18 min instead of 14 min. Lowering the KPS concentration to 0.32 mM further slows the rate

and almost twice as long is needed to reach complete conversion.

The diameter of the final latex particle is around 80 nm and does not depend on initiator concentration. The final average molecular weight of the polymer depends only slightly on the initiator concentration, but the average molecular weight decreases and the polydispersity ( $\bar{M}_w/\bar{M}_n$ ) increases as function of conversion for all three reactions (Table 1).

**Effect of composition:** Adding relatively large amounts of NaBr into the mixtures allows the solubilization of higher monomer concentrations (see Fig. 2). Polymerizing a mixture with  $\alpha = 5$  wt% at  $\varepsilon = 10$  wt% causes polymer to precipitate at 40% conversion. Lowering the electrolyte amount to  $\varepsilon = 2.27$  wt% (0.25 M) NaBr with  $\alpha = 1.5$  wt% leads to polymer precipitation during the reaction after 60% conversion. The mixture remains stable and bluish during the reaction when only 0.05 M NaBr (with  $\alpha = 1.5$  wt%) is used. Within the error bars of the experiment, the reaction rate and final latex particle diameter do not change with added salt (Fig. 3b and Table 1). The molecular weight decreases as function of conversion as observed previously. However,  $\bar{M}_w$  is approximately 30% less than  $\bar{M}_w$  for the polymer produced in the salt-free mixture.

Changing the oil concentration from  $\alpha = 1.50$  wt% to 1.00 wt% also has little effect on the reaction rate (Fig. 3b). The initiator concentration based on the oil content is the same in both cases but the reduction in oil concentration changes the overall initiation concentration from 1.64 to 1.08 mM. The conversion curves are identical during the first 10 min of the reaction, then the rate decreases and the reaction reaches a slightly lower conversion for the system containing less monomer. The polymer formed has a more polydisperse molecular weight distribution and a lower average molecular weight ( $\bar{M}_w = 7 \times 10^5$  compared to  $\bar{M}_w = 1.6 \times 10^6$  for the  $\alpha = 1.50$  wt% microemulsion). The overall change in average molecular weight during the reaction is low (Table 1).

#### Styrene system

C6MA and styrene have almost identical phase behaviour (Fig. 2) although more styrene (up to ca. 1 wt%) is soluble in formamide with no surfactant present. Figure 4 shows the conversion curves for the system containing C6MA and styrene at  $\alpha = 1.00$  wt%. The initiator concentration was 1.08 mM and 3.18 mM for C6MA and styrene polymerizations respectively. Even though the styrene polymerization had a higher initiator concentration, the reaction reaches a conversion of 83% after ca. 5 h (97% after 10 h), whereas the C6MA reaction reaches high

**Table 1** Polymer and reaction summary

System	$\alpha$ (wt%)	KPS (mM)	Conversion (%)	Dia. (nm)	$\bar{M}_w (\times 10^6)$	$\bar{M}_w/\bar{M}_n^a$
Styrene	1.00	3.18	45	—	0.107	M
			62	—	0.092	M
			83	—	0.073	M
			95	—	0.074	M
			97	75	0.066	M
C6MA	1.50	3.18	40	—	1.51	1.18
			68	—	1.27	1.25
			86	—	1.11	1.37
			90	—	1.10	1.40
			98	88	1.11	1.84
		1.64	40	—	2.26	1.15
			66	—	1.99	1.29
			77	—	1.88	1.30
			93	—	1.69	1.40
			99	—	1.59	1.76
	1.00	1.08	48	—	2.20	1.13
			62	—	2.03	1.23
			78	—	1.85	1.33
			88	—	1.78	1.37
			99	76	1.52	1.45
		0.32	35	—	2.11	1.20
			66	—	1.80	1.21
			85	—	1.69	1.26
			95	—	1.64	1.28
			98	80	1.66	1.40
Salt	1.50	1.64	61	—	1.29	1.16
			73	—	1.27	1.17
			90	—	1.15	1.25
			94	—	1.12	1.21
			99	78	1.09	1.34

<sup>a</sup> Polydispersity reported only for samples displaying one peak. M indicates multimodal sample.

conversion (95%) in about 20 min and a final conversion of 98% is reached after 34 min.

The final average molecular weight of the polystyrene formed is 10 times lower than that of polyC6MA (Table 1). In addition, the polystyrene has a much broader molecular weight distribution than polyC6MA. A qualitative measure of the polydispersity can come from comparing the concentration responses of the refractive index detector as function of time for the two polymers (Fig. 5). A typical spectrum for a rather monodisperse polyC6MA is shown as curve **a** (for a microemulsion with  $\alpha = 1.50$  wt%). Curve **b** shows how the spectrum becomes bimodal as the oil concentration is decreased to  $\alpha = 1.00$  wt%. Spectra **c** shows that the polystyrene formed at  $\alpha = 1.00$  wt% is multimodal and polydisperse, and elutes over a broad range of time.

## Discussion

We begin with sample preparation. Oxygen is a free radical scavenger [25], so its presence in free radical reaction mixtures either retards or inhibits the initiator–monomer reaction. The presence of oxygen generally results in an induction period after the initiator is added to the solution. Some authors mention the presence of an induction period, and set the observed increase in conversion as the starting point of their reaction. Others present the induction period in their graphs, whereas some do not mention induction periods. Although all groups use some kind of technique to remove oxygen from the solution, there is unfortunately no easy method to determine the total oxygen concentration in the solution. However, using

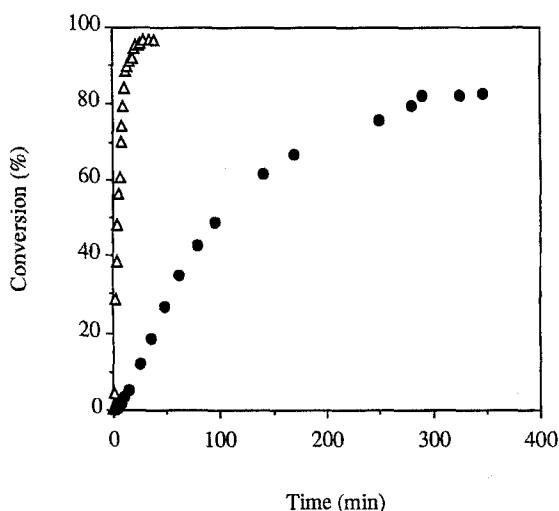


Fig. 4 Conversion as a function of time for the microemulsion polymerization at  $T = 60^\circ\text{C}$  of ( $\Delta$ )  $\alpha = 1.0$  wt% C6MA with 1.08 mM KPS; ( $\bullet$ )  $\alpha = 1.0$  wt% styrene with 3.18 mM KPS

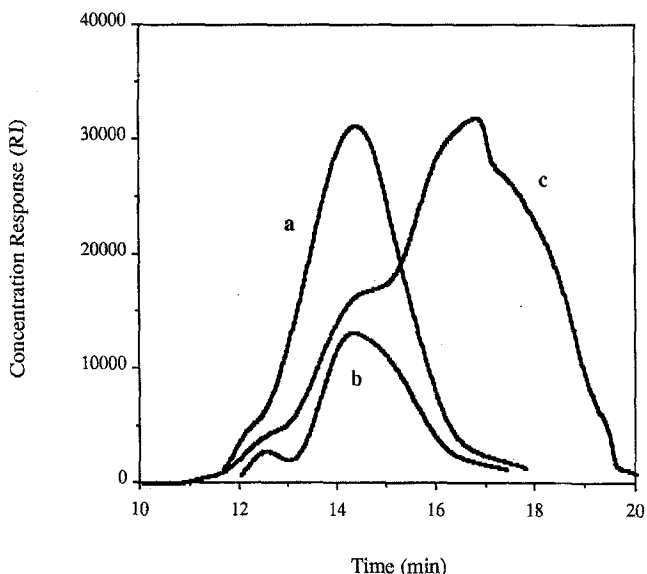


Fig. 5 Concentration responses of the RI detector (SEC) for (a)  $\alpha = 1.5$  wt% C6MA (b)  $\alpha = 1.0$  wt% C6MA and (c)  $\alpha = 1.0$  wt% styrene

a freeze-thaw technique to remove dissolved oxygen is known to be efficient and allows consistent and reproducible results. All the conversion curves presented here demonstrate that the amount of oxygen present in these samples must be low because no induction period is observed.

#### Phase behavior

A goal of this study is to investigate the phase behavior of polymerizable nonaqueous microemulsions systematically

using the least number of components possible. Using formamide instead of water allows systematic phase behavior studies in a quaternary mixture at constant temperature. Obtaining the "fish" diagram (see Fig. 1) for mixtures containing equal amounts of water and oil – although no reaction is carried out in such a system – provides key information about the system; see e.g., Kahlweit et al. [35]. In addition, the "fish" diagram gives information about if and what microstructures are formed (see [31] and references therein). A rule of thumb is that if microemulsions form with such equal weight (volume) mixtures, then a channel cut gives information about the extension of the microemulsion region at constant surfactant concentration. This was examined at 10 wt% total surfactant concentration (see Fig. 2). The phase diagrams for both monomers are almost identical, although their solubility in formamide is different. This makes these reacting microemulsions unique because monomers with different solubilities in the continuous phase can be polymerized under identical conditions.

#### Polymerization

Polymerization reactions in these nonaqueous microemulsions lead to stable, bluish dispersions of latex particles. The amount of initiator used here is relatively high, ranging from 0.32 mM to 3.18 mM, as compared to aqueous systems where typically 0.15 mM to 0.60 mM of initiator is used. Based on the weak dependence of the rate on initiator concentration, it is likely that lower amounts of KPS might still lead to high conversion in a short period of time. Of course, formamide is not water, and solvent effects are important in free radical chemistry (for a review see ref. [41]). Thus the decomposition rate of the initiator is probably different in formamide than in water, and the cage effect [42] may alter the initiator efficiency because formamide itself is a conjugating system that forms a zwitterion.

During the reaction there is a linear decrease of the average molecular weight of the polymer as a function of conversion (and an increase in polydispersity,  $\bar{M}_w/\bar{M}_n$ ). This suggests that the dominant mode of termination is *not* chain transfer to monomer, which would result in a constant  $\bar{M}_w$  during the polymerization [43, 44]. The propagation rate is proportional to the monomer concentration in the latex particle and thermodynamic modeling shows that the monomer equilibrium concentration decreases linearly with conversion in microemulsion polymerization [45]. So only if the termination rate is independent of monomer concentration in the polymer particle and remains constant throughout the reaction would one expect a decrease in the average molecular

weight with conversion. One such termination mode would be second entry of a free radical into the polymer particle causing instantaneous combination with the growing chain. Over the time frame of the reaction, the entry rate [46] remains constant. If multiple entry instead of chain transfer to monomer is the dominant termination mechanism, one would expect to find more than the one to three chains per particle resulting from chain-transfer limited microemulsion polymerizations [43, 44]. In the nonaqueous polymerizations in this study, latexes with diameters of 80 nm containing polymers of  $\bar{M}_w \sim 1 \times 10^6$  have approximately 160 chains per particle, which is consistent with a multiple entry mechanism.

Changing the composition of the parent microemulsion system and studying the resulting polymerization rate provides more insight to the role the non-reacting components might play. The addition of bromide ions, for example, is expected to inhibit the polymerization reaction because the sulfate free radical reacts with the bromide ion to produce neutral bromide radicals which do not initiate the polymerization reaction [47]. The rate constant for this reaction is larger than that for radical reaction with styrene monomer (it is probably comparably high for C6MA), and so the bromide ions should quench the reaction. The system we studied here contained 50 mM bromide ions and 3.28 mM sulfate radicals (assuming total decomposition of the initiator) and the reaction proceeded at the same rate as the system without NaBr. Thus, bromide is not inhibiting the polymerization reaction at these concentrations.

Polymerizing a mixture that contains lower amounts of oil (at constant surfactant concentration) showed a dramatic effect on the average molecular weight (see Table 1) but only a minor effect on the reaction rate (Fig. 3b). The literature points to a similar trend in molecular weight decrease [15, 26, 48–52], although again, direct comparison is difficult because in the referenced studies changes of oil content were accompanied by changes in the cosurfactant or surfactant concentration.

Exchange of styrene for C6MA shows that despite almost identical phase behavior (Figs. 1 and 2), the two monomers have very different polymerization rates (Fig. 4) and final polymer properties (Fig. 5). The polymerization of styrene reflects more of the features of solution polymerization (a long reaction time resulting in low molecular weights with a polydisperse distribution). Relatively low molecular weights with a bimodal population were formed in the case of the microemulsion containing 1 wt% of C6MA. Both of these observations point to the fact that the solubility of the oil in the polar solvent plays an important role in determining the final polymer character-

istics. The reason for such a drastic change in average molecular weight might be that the relative amount of monomer in the polar domain increases. Let  $R$  be the ratio of monomer solubilized in the micelle to monomer soluble in the continuous polar phase. If the monomer solubility in the polar phase is constant even with surfactant present (which is sufficient for a qualitative argument),  $R$  changes from 6.5 to 4 when the amount of C6MA is lowered from  $\alpha = 1.50$  wt% to  $\alpha = 1.00$  wt%. In this case, the average molecular weight of the polymer decreases by about 50%. In the styrene polymerization,  $R = 0$ , which is the case of a solution polymerization with empty micelles present, and yields a very polydisperse low molecular weight polymer. Initiation of the monomer occurs in the polar domain because the sulfate radical is solvophilic. After a critical oligomer size is reached, the propagating chain becomes solvophobic enough to enter the micelle. However, if the micelles contain no monomer, propagation is slow and the polymer formed is of low molecular weight. The situation is different when C6MA is substituted because the propagating chain enters a micelle that contains a solubilized reservoir of monomer, allowing the chains to grow to a higher molecular weight before a termination event occurs. Additionally, differences in glass transition temperatures for the polymers (the  $T_g$  of poly-C6MA is  $-5^\circ\text{C}$ , while that of polystyrene is  $100^\circ\text{C}$ ) could also play a role because the growing polystyrene chain is stiff while the poly-C6MA chain is flexible.

## Conclusion

Microemulsion formation occurs in a nonaqueous system containing either styrene or hexyl methacrylate. Nonaqueous systems with formamide as the water substitute are well suited for systematic phase behavior studies because ionic surfactants form microemulsions in either ternary or quaternary systems at constant temperature. We found identical phase behavior in microemulsions regardless of the oil, although the oil solubility in the continuous phase differs significantly. Nonaqueous microemulsions can be polymerized at fast reaction rates, yielding stable, bluish latices. Minor changes in composition can have large effects on reaction rates and on the characteristics of the final polymer. All reactions showed decreasing average molecular weight as function of conversion, indicating that the ratio of the propagation rate to the termination rate decreases during the polymerization. The solubility of the monomer in the polar domain plays an important role and determines the characteristics of the final latex.



## References

1. Martino A, Kaler EW (1990) *J Phys Chem* 94:1627–1631
2. Martino A, Kaler EW (1995) *Langmuir* 11:779–784
3. Schubert K-V, Busse G, Strey R, Kahlweit M (1993) *J Phys Chem* 97:248–254
4. Stoffer JO, Bone T (1980) *J Polym Sci: Polym Chem Edn* 18:2641–2648
5. Stoffer JO, Bone T (1980) *J Dispersion Sci Technol* 1:37–54
6. Atik SS, Thomas JK (1981) *J Am Chem Soc* 103:4279–4280
7. Atik SS, Thomas JK (1982) *J Am Chem Soc* 104:5868–5874
8. Atik SS, Thomas JK (1983) *J Am Chem Soc* 105:4515–4519
9. Gan LM, Chew CH, Friberg SE (1983) *J Macromol Sci Chem* A19:739–756
10. Candau F (1992) In: Paleos CM (ed) *Polymerization in Organized Media*. Gordon and Breach Science Publishers, Philadelphia, pp 215–282
11. Jayakrishnan A, Shah DO (1984) *J Polym Sci: Polym Lett Edn* 22:31–38
12. Haque E, Qutubuddin S (1988) *J Polym Sci: Part C: Polym Lett Edn* 26:429–432
13. Bléger F, Murthy AK, Pla F, Kaler EW (1994) *Macromolecules* 27:2559–2565
14. Full AP, Puig JE, Gron LU, Kaler EW, Minter JR, Mourey TH, Texter J (1992) *Macromolecules* 25:5157–5164
15. Guo JS, El-Aasser MS, Vanderhoff JW (1989) *J Polym Sci: Part A: Polym Chem Edn* 27:691–710
16. Strey R, Jonströmer M (1992) *J Phys Chem* 96:4537–4542
17. Johnson PL, Gulari E (1984) *J Polym Sci: Polym Chem Edn* 22:3967–3982
18. Tang H-I, Johnson PL, Gulari E (1984) *Polymer* 25:1357–1362
19. Guo JS, El-Aasser MS, Sudol ED, Yue HJ, Vanderhoff JW (1990) *J Colloid Interf Sci* 140:175–184
20. Gan LM, Chew CH, Lye I, Ma L, Li G (1993) *Polymer* 34:3860–3865
21. Kahlweit M, Strey R, Busse G (1991) *J Phys Chem* 95:5344–5352
22. Guo JS, Sudol ED, Vanderhoff JW, Yue HJ, El-Aasser MS (1992) *J Colloid Interf Sci* 149:184–196
23. Kahlweit M, Strey R, Busse G (1993) *Phys Rev E* 47:4197–4209
24. Kahlweit M (1995) *J Phys Chem* 99:1281–1284
25. Odian G (1991) *Principles of Polymerization*. John Wiley & Sons Inc, New York
26. Perez-Luna VH, Puig JE, Castano VM, Rodriguez BE, Murthy AK, Kaler EW (1990) *Langmuir* 6:1040–1044
27. Puig JE, Perez-Luna VH, Perez-Gonzales M, Macias ER, Rodriguez BE, Kaler EW (1993) *Colloid Polym Sci* 271:114–123
28. Rodriguez-Guadarrama LA, Mendizabal E, Puig JE, Kaler EW (1993) *J Appl Polym Sci* 48:775–786
29. Antonietti M, Bremser W, Müschenborn D, Rosenauer C, Schupp B (1991) *Macromolecules* 24:6636–6643
30. Antonietti M, Lohmann S, Van Niel C (1992) *Macromolecules* 25:1139–1143
31. Lusvardi KM, Kaler EW (1995) *Langmuir* 11:4728–4734
32. Jonströmer M, Sjöberg M, Wärnheim T (1990) *J Phys Chem* 94:7549
33. Schubert K-V, Kahlweit M, Strey R (1992) In: Friberg SE, Lindman B (eds) *Organized Solutions*. Marcel Dekker, New York, pp 105–114
34. Firman P, Haase D, Jen J, Kahlweit M, Strey R (1985) *Langmuir* 1:718–724
35. Kahlweit M, Strey R et al (1987) *J Colloid Interf Sci* 118:436–453
36. Shinoda K, Lindman B (1987) *Langmuir* 3:135–149
37. Kahlweit M, Strey R, Schomäcker R (1989) In: Knoche W and Schomäcker R (eds) *Reactions in Compartmentalized Liquids*. Springer-Verlag, Berlin, pp 1–10
38. Landolt-Börnstein (1964) In: Schaëfer K, Lax E (eds) *Zahlenwerte und Funktionen*, Vol 2.2c. Springer-Verlag, Berlin, p 674
39. Stephen H, Stephen T (1963) *Solubilities*, Vol 1.1. Oxford University Press, Oxford, p 432
40. Vijayendran BR (1979) *J App Polym Sci* 22:733–742
41. Martin JC (1973) In: Kochi JK (eds) *Free Radicals*. John Wiley & Sons, New York, pp 493–524
42. Franck J, Rabinowitch F (1934) *Trans Faraday Soc* 30:120
43. Full AP, Kaler EW, Arrellano J, Puig JE (1996) *Macromolecules* 29:2764–2775
44. Full AP (1994) Ph.D. Dissertation, University of Delaware
45. Guo JS, Sudol ED, Vanderhoff JW, El-Aasser MS (1992) *J Polym Sci: Part A: Polym Chem Edn* 30:691–702
46. Maxwell IA, Morrison BR, Napper DH, Gilbert RG (1991) *Macromolecules* 24:1629–1640
47. Neta P, Hule RE, Ross AB (1988) *J Phys Chem Ref Data* 17:1027–1238
48. Feng L, Ng KYS (1990) *Macromolecules* 23:1048–1053
49. Gan LM, Chew CH, Lye I (1992) *Makromol Chem* 193:1249–1260
50. Gan LM, Chew CH, Lye I, Imae T (1991) *Polym Bull* 25:193–198
51. Gan LM, Chew CH, Lee KC, Ng SC (1993) *Polymer* 34:3064–3069
52. Gan LM, Chew CH, Ng SC, Loh SE (1993) *Langmuir* 9:2799–2803